FAN-STRUCTURE DYNAMIC SHEAR RUPTURE MECHANISM GENERATED IN INTACT HARD ROCKS AT HIGHLY CONFINED COMPRESSION

Boris G. TARASOV[1]

ABSTRACT

Frictional shear resistance along pre-existing faults is considered to be the lower limit on rock shear strength at confined compression corresponding to the seismogenic layer. This determines the lithospheric strength and the primary earthquake mechanism associated with frictional stick-slip instability on pre-existing faults. This paper proposes a new approach in understanding of the lithospheric strength and earthquake activity on pre-existing faults on the basis of a recently identified fan-structure dynamic shear rupture mechanism activated in hard rocks at highly confined compression. A paradoxical feature of this mechanism is the ability to develop new dynamic faults in intact rock mass at shear stress levels significantly less than frictional strength. Another important feature is that for the initial formation of the fan-structure (representing the head of propagating fault) an enhanced local shear stress is required. Accoring to the new approach pre-existing discontinuities in the Earth's crust play the role of local stress concentrators providing the initial formation of the fan-head in the adjoining intact rock mass. Further dynamic creation of a large new fault (earthquake) can occure at low shear stresses even below the frictional stregnth. Paradoxically low strength of intact rock provided by the fan-mechanism favours the generation of new faults in the intact rock mass adjoining the pre-existing fault in preference to frictional stick-slip instability along the pre-existing fault. The varying efficiency of the fan-mechanism with depth provides a specific depth distribution of lithospheric strength and earthquake activity.

INTRODUCTION

Earthquakes are normally related to pre-existing discontinuities (e.g. faults, boundaries between tectonic plates), which implies an essential role of them in earthquake activity. Modern understanding of the nature of earthquakes is that the primary mechanism comprises stick-slip instability on pre-existing faults, along which the frictional strength represents a lower limit on rock shear strength in the lithosphere (Scholz, 2002). Depth distribution of the lithospheric shear strength within the seismogenic layer is determined by the Byerlee's law (Byerlee, 1978) in consideration of enhanced temperature at great depths (Brace and Kohlstedt, 1980).

This paper proposes a new approach in understanding of earthquake activity on pre-existing discontinuities based upon a recently identified fan-structure dynamic shear rupture mechanism (Tarasov, 2010; Tarasov and Randolph, 2011; Tarasov and Guzev, 2013; Tarasov, 2014). The fan-mechanism is activated in intact hard rocks (characterised by uniaxial compressive stregnth above 250 MPa) at highly confined compression corresponding to the seismogenic layer. A paradoxical feature of the fan-mechanism is the ability to develop new dynamic faults in intact rock mass at shear stress

---

[1] Professor, The University of Western Australia, Perth, boris.tarasov@uwa.edu.au

levels significantly less than frictional strength. However, for the initial formation of the fan-head a high local shear stress is required. The paper proposes that in nature the fan-mechanism can be activated mainly in the proximity to pre-existing discontinuities which play the role of local stress concentrators providing high stresses in the adjoining intact rock mass necessary for the initial formation of the fan-head. Further dynamic creation of a new large fault (earthquake) can occur at low shear stresses even below the frictional stregnth. According to the new approach, paradoxically low strength of intact rock provided by the fan-mechanism favours the generation of new faults in the intact rock mass surrounding the pre-existing fault in preference to frictional stick-slip instability along the pre-existing fault. However, the proximity of the pre-existing faults to the area of instability caused by the fan-mechanism creates the illusion of stick-slip instability on the pre-existing faults, thus concealing the real situation. The varying efficiency of the fan-mechanism with depth provides a specific depth distribution of lithospheric strength and earthquake activity. This question is also discussed in the paper.

CONVENTIONAL AND UNCONVENTIONAL POST-PEAK ROCK BEHAVIOUR AT CONFINED COMPRESSION

In laboratory experiments on rock specimens a macroscopic instability associated with strength degradation due to spontaneous rock failure can only take place in the post-peak region. The post-peak instability can be treated as a manifestation of rock brittleness. Recent studies of post-peak failure of hard rocks (characterised by uniaxial compressive strength UCS > 250 MPa) at highly confined compression ($\sigma_1 > \sigma_2 = \sigma_3$) showed very specific their behaviour at these testing conditions (Tarasov, 2010; Tarasov and Randolph, 2011; Tarasov, 2014).
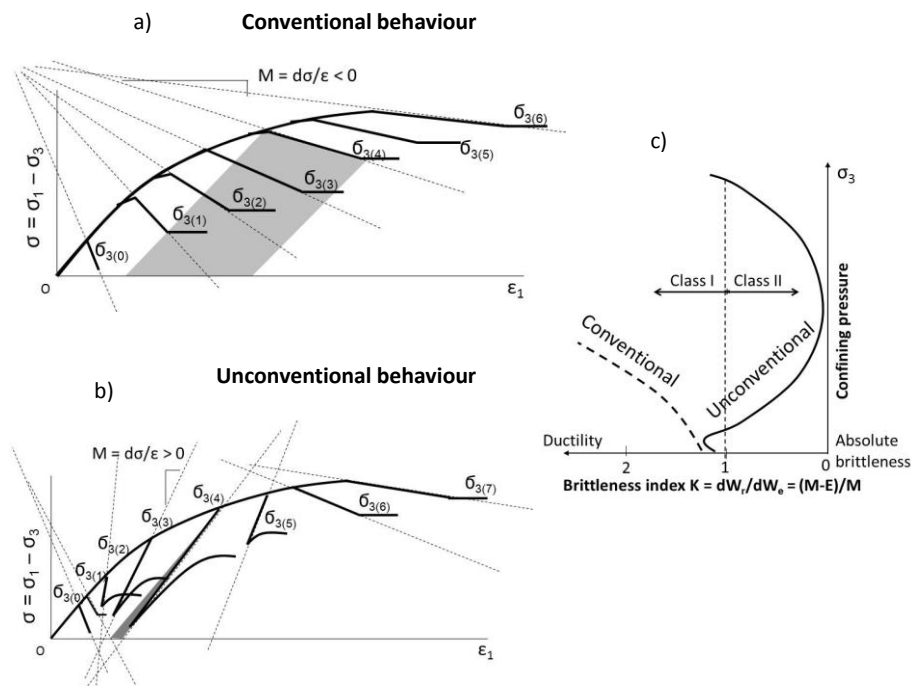

Figure 1. Two sets of generic stress-strain curves for different levels of confining pressure σ_3 illustrating a) conventional and b) unconventional rock behaviour. c) Typical variation of the post-peak brittleness index K with rising σ_3 for rocks exhibiting the conventional and unconventional behaviours

Fig. 1 shows two sets of generic stress-strain curves for different levels of confining pressure σ_3. Fig. 1a represents the conventional (well-studied) rock behaviour associated with increasing post-peak ductility with rising σ_3. To clearly show the character of variation of the post-peak curves they are indicated by dotted lines. The conventional behaviour is typical for relatively soft rocks. Fig. 1b represents the unconventional type of behaviour typical for hard rocks. Here increasing σ_3 can lead to a contradictory variation of post-peak properties. In fact, rock behaviour can be changed from Class I

to extreme Class II and then to Class I again. Class I is characterised by negative post-peak modulus M = dσ/dε, while Class II by positive (Wawersik and Fairhurst, 1970). At extreme Class II values of post-peak modulus M and elastic modulus E = dσ/dε can be very close indicating extremely small post-peak rupture energy (compare shaded areas in Fig. 1a and 1b for $\sigma_3 = \sigma_{3(4)}$).

Small post-peak rupture energy in turn indicates high post-peak brittleness. A special brittleness index was developed to characterise unambiguously the post-peak brittleness at any type of rocks behaviour (see details in Tarasov and Potvin, 2013). The index K = dW$_r$/dW$_e$ = (M - E)/M is based on the ratio between the post-peak rupture energy dW$_r$ and elastic energy dW$_e$ withdrawn from the material during the failure process. The index K characterises the capability of the rock for self-sustaining failure due to the elastic energy available from the failing material. Fig. 1c shows variation of the brittleness index K with rising confining pressure σ_3 for rocks exhibiting the conventional and unconventional behaviour. In contrast to the conventional behaviour where rising σ_3 is accompanied by a monotonic decrease in post-peak brittleness, the brittleness variation for unconventional behaviour follows a typical pattern of initially increasing, reaching a maximum and then ultimately decreasing. The harder the rock, the greater the effect of embrittlement. Experiments (Tarasov, 2010) showed that some rocks at high confinement became hundreds of times more brittle compared to uniaxial compression approaching the absolute brittleness. The absolute brittleness has the following characteristics and parameters:

- The post-peak rupture energy is equal to zero dW$_r$ = 0,
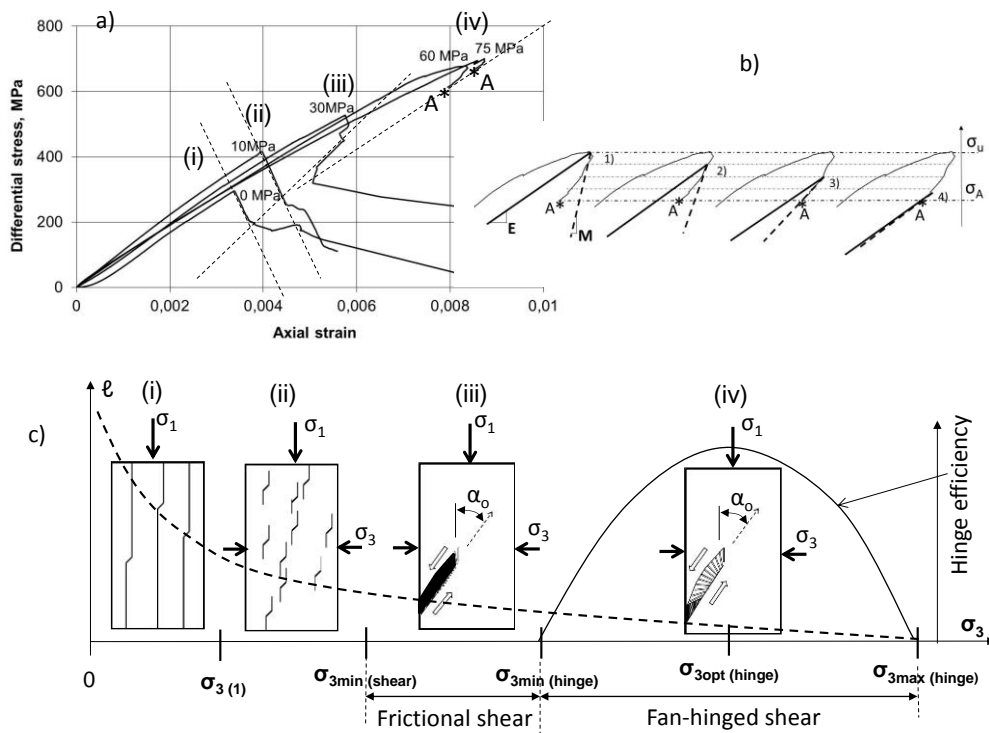- The post-peak modulus is the same as the elastic modulus M = E,
- K = 0.

Figure 2. Variation in failure mechanisms and failure patterns with σ_3 for rocks exhibiting the unconventional post-peak behaviour

Fig. 2 illustrates one more extremely important feature of the unconventional behaviour exhibited by hard rocks with UCS > 250 MPa and a failure mechanism responsible for that. Fig. 2a shows a set of stress-strain curves obtained on dolerite specimens (UCS = 300 MPa) at different levels of σ_3. The testing was conducted on an extremely stiff and servo-controlled testing machine based upon the loading principles described in Stavrogin and Tarasov (2001). It is typical for hard rocks that within a special range of high confining pressure (different for different rocks) post-peak control is possible only at the start of the post-peak stage only after which spontaneous and very violent failure is followed. For the dolerite the uncontrollable failure took place at $\sigma_3 \geq 60$ MPa. The maximum level

of confining pressure in experiments was $\sigma_3 = 200$ MPa. In Fig. 2a points A of the instability start for $\sigma_3 = 60$ and 75 MPa are indicated by asterisks. It is important to note that with rising confining pressure the controllable post-peak stage decreases (compare curves for $\sigma_3 = 60$ and 75 MPa). At higher σ_3 the controllable post-peak stage became very small.

Fig. 2b explains the reason why the post-peak control becomes impossible after point A. It shows an enlarged fragment of the stress-strain curve for $\sigma_3 = 60$ MPa involving the post-peak part at stress degradation from ultimate stress σ_u till σ_A (this fragment is replicated four times). The post-peak curves divided into four stages with equal intervals of differential stress. Each stage is characterised by average values of elastic modulus E (solid lines) and post-peak modulus M (dotted lines). Areas located between the E and M lines indicate the current post-peak rupture energy dW_r:

$$dW_r = \frac{(\sigma_o^2 - \sigma_e^2)(M - E)}{2ME}$$

Here σ_o and σ_e are differential stresses at the onset and the end of each stage.

We can see that the current post-peak rupture energy decreases dramatically with the rupture development from stage 1 to stage 4. At stage 4 the rupture energy becomes extremely small because modulus *M* approaches modulus *E*. At point A the lines indicating modulus M and E practically coincide and post-peak control becomes impossible.

Fig. 2c illustrates evolution of failure mechanisms in hard rocks with rising confining pressure σ_3 (from left to right) which causes a specific variation in post-peak behaviour. It is known that in brittle rocks pre-existing defects at loading generate tensile cracks the ultimate length ℓ of which is a function of σ_3 as shown symbolically by a dotted line: the higher σ_3 the shorter ℓ. The length ℓ of tensile cracks in turn determines the macroscopic failure mechanism and the failure pattern shown in rectangles representing rock specimens.

At confining pressures $0 \leq \sigma_3 < \sigma_{3min(shear)}$ shear rupture cannot propagate in its own plane due to creation in the rupture tip of relatively long tensile cracks preventing the shear rupture development. The tensile cracks grow along the major stress. Two failure mechanisms distinguished at these stress conditions are: (i) splitting by long tensile cracks and (ii) failure due to coalescence of distributed micro-cracks accumulated within the material body during loading. The first mechanism is typical for uniaxial compression $\sigma_3 = 0$ and the second one for low confining pressures (e.g. $\sigma_3 = 0$ and 10 MPa for dolerite in Fig. 2a).

At $\sigma_3 \geq \sigma_{3min(shear)}$ the failure mode is the localized shear. Due to high confinement micro tensile cracks become sufficiently short to cause shear rupture to propagate in its own plane. Here the dilation of one short micro-crack induces the dilation of closely spaced neighbouring crack (Reches and Lockner, 1994). Due to consecutive creation of short tensile cracks in front of the rupture tip the advancing fault itself induces organized damage which is restricted to its own plane. It is important to note that micro-cracks are generated along the major stress which is at angle $\alpha_o \approx (30^o \div 40^o)$ to the shear rupture plane (Reches and Lockner, 1994; Horii and Nemat-Nasser, 1985). This micro-cracking process creates inclined intercrack blocks (known as domino-blocks) which are subjected to rotation at shear displacement of the rupture interfaces (Peng and Johnson, 1972; King and Sammis, 1992; Reches and Lockner, 1994). Two specific shear rupture mechanisms have been distinguished here.

(iii) *Frictional shear*. This mechanism is associated with collapse of domino-blocks at rotation and creation of friction in the shear rupture interface (Peng and Johnson, 1972; King and Sammis, 1992; Reches and Lockner, 1994). For hard rocks this mechanism can operate within the pressure range $\sigma_{3min(shear)} < \sigma_3 < \sigma_{3min(hinge)}$. Shear rupture development governed by this mechanism can be controlled on stiff and servo-controlled testing machines (curve for $\sigma_3 = 30$ MPa in Fig. 2a).

(iv) *Fan-hinged shear*. This mechanism is generated in hard rocks (characterised by UCS > 250 MPa). Further increases of the confining pressure above $\sigma_3 = \sigma_{3min(shear)}$ will continue reducing the length ℓ of tensile cracks (dotted curve in Fig. 2c) and, consequently, the length of domino-blocks composing the fault structure. Due to very strong material and proper geometry of short domino-blocks within the range $\sigma_{3min(hinge)} < \sigma_3 < \sigma_{3max(hinge)}$ they can withstand rotation caused by the shear displacement of the rupture faces without collapse. In this case the domino-blocks behave as hinges decreasing dramatically friction between the rupture faces. Due to consecutive generation and rotation

of the domino-blocks they create a fan-structure representing the shear rupture head. The fan-head has different extraordinary features causing uncontrollable and violent shear rupture development (curves for $\sigma_3 = 60$ and 75 MPa in Fig. 2a).

It should be emphasized that the efficiency of the fan-mechanism is variable and determined by how perfect the fault structure is. The solid curve in Fig. 2c shows symbolically the variation of the fan-mechanism efficiency versus confining pressure. The variable efficiency of the fan-mechanism determines corresponding variation of the post-peak rock brittleness (see Fig. 1c) and shear resistance of the fan-head. This question will be discussed further.

EXTRAORDINARY FEATURES OF THE FAN-MECHANISM

Physical and mathematical models of the fan-mechanism discussed in Tarasov and Guzev (2013), Tarasov (2014) demonstrate that the fan-head combines such unique features as: extremely low shear resistance (significantly below the frictional strength), self-sustaining stress intensification in the rupture tip, and self-unbalancing conditions. Due to this the failure process caused by the fan-mechanism is very dynamic and violent which destroy the initial fault structure creating pulverized gouge. This makes it impossible to directly observe and study the fan-mechanism in laboratory and in nature and can explain why the mechanism has not been detected before. Physical motivation for the fan-mechanism based upon side effects accompanying the failure process was provided in Tarasov (2014).

The physical model in Fig. 3 illustrates the most intriguing features of the fan-mechanism. As mentioned above shear ruptures propagate through rocks due to consecutive formation of identical domino-blocks from the intact material in the rupture tip. Further rotation of the blocks between the shear rupture faces can lead to frictional shear (at block collapse) or to fan-hinged shear (at block rotation without collapse). The mechanism responsible for the creation of identical domino-blocks is not discussed in the developed physical and mathematical models. In the models the domino-blocks are considered as 'predetermined' and operated with optimal efficiency (without collapse at rotation). The models discuss the influence of the fan-structure formed on the basis of rotating blocks on the rupture process.
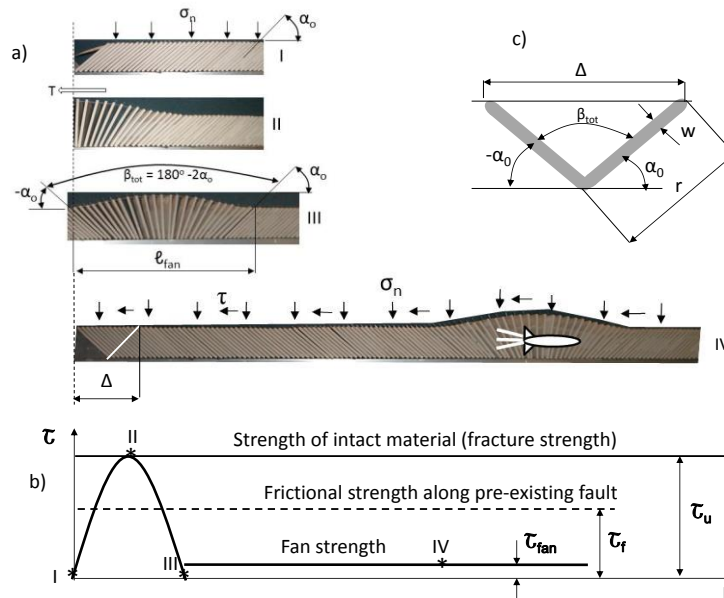

Figure 3. a) Photographs illustrating the fan-structure at different stages of its formation. b) Variation in shear resistance of the fan-structure during its formation and propagation. c) A domino-block at the initial and final positions.

Photographs of the physical model in Fig. 3 show different stages of the fan-mechanism operation. At the initial condition (Fig. 3a-I) a row of identical domino-blocks inclined at angle α_0 represents an implicit horizontal shear rupture (fault). Surfaces of neighbouring domino-blocks are in full contact providing a very compact "monolithic" material. To simulate the resistance of domino-blocks to tearing-off from the monolithic material (which takes place in real materials) the blocks are bonded to each other. The row of domino-blocks is located between two layers of elastic material (elastic connectors) representing the fault interfaces. The upper and lower elastic connectors are fixed to corresponding ends of each domino-block. Contact areas between the ends of domino-blocks and the interfaces we will call joints. As such a version of the model with bonded blocks can be treated as representing an intact material. Evenly distributed weight located on the upper layer creates normal stress applied to the simulated fault σ_n.

For initial formation of the fan-structure a local stress should be applied as illustrated by the graph in Fig. 3b. During this process shear resistance of the developing fan-head is variable: initially it increases and reaches a maximum value when the first half of the fan-structure has completed (Fig. 3a-II). Shear resistance at this moment corresponds to the material strength τ_u. The totally completed fan-structure (Fig. 3a-III) is self-balancing and shear resistance of it is extremely small.

To make the fan-structure self-unbalancing a distributed shear stress τ should be applied to the whole domino row. Under the effect of the distributed shear stress the fan propagates spontaneously along the whole row as a wave sequentially moving the loaded upper face against the lower one by distance Δ (see Fig. 3a-IV). Experiments on the physical model and analysis of the mathematical model in Tarasov and Guzev (2013), Tarasov (2014) demonstrated that the fan-structure causes self-sustaining stress intensification in the rupture tip which assists in creation of new domino-blocks in the rupture tip providing easy propagation of the fan-head through the intact material. It was shown that shear resistance of the propagating fan-head is extremely small and determined only by friction in joints of rotating domino-blocks and their geometry (Eq. 1):

$$\tau_{fan} = 0.85\tau_f \frac{w}{r}$$

(1)

Hear, τ_{fan} is the shear resistance of the fan-head; τ_f is the sliding friction; w is the width and r is the length of domino-blocks (see Fig. 3c showing a domino-block in the initial and final positions).

It was established that shear resistance of the fan-structure τ_{fan} can be significantly (up to ten times) less than the conventional frictional resistance τ_f between the fault surfaces at the absence of domino-blocks: $\tau_{fan} \approx 0.1\tau_f$. In Fig. 3b the horizontal lines indicate three levels of stresses: fracture material strength τ_u, frictional strength τ_f, and fan-structure strength τ_{fan}. It should be emphasized that the low resistance of the sleeping rupture surfaces takes place within the zone of the moving fan-head only. In front of the fan the material is in an intact condition. Behind the fan shear resistance is equal to friction. Due to this the fan-mechanism provides the pulse-like rupture mode: at any given time during rupture propagation, slip occurs over only a narrow band (fan-head) along the fault and the fault relocks behind the rupture head. This slip pulse propagates forward as the fault proceeds. Pulse-like rupture mode was observed for earthquakes (Heaton, 1990) and in laboratory (Ohnaka et al., 1986; Lykotrafitis et al., 2006). A video illustrating the fan wave propagation along the domino row of the physical model can be seen in Tarasov (2014).
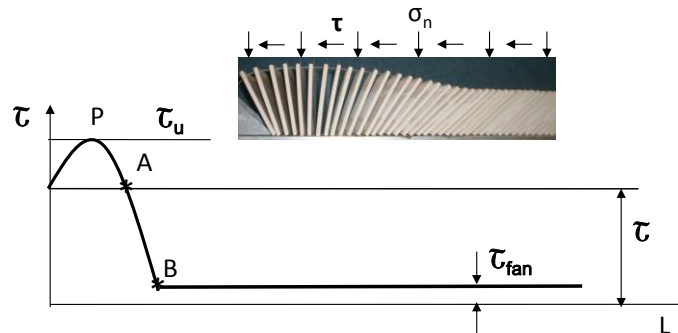

Figure 4. Principle of instability generation before the completion of the fan-structure

It is important to note that if we develop the fan-structure by application of a local stress in a domino row, which was loaded earlier by a distributed shear stress above the fan-structure strength ($\tau > \tau_{fan}$), the instability will start before the completion of the fan-structure. Fig. 4 illustrates this situation. The horizontal lines on the graph here indicate levels of the material strength τ_u, distributed shear stress τ applied along the domino row and the fan-structure strength τ_{fan}. In this situation stable formation of the fan-structure will take place until point A has been reached. After point A shear resistance of the uncompleted fan-structure becomes lower than the applied distributed shear stress, which will cause instability. The rest part of the fan will be formed dynamically and the completed fan-head will continue propagating spontaneously along the row. A photograph of the uncompleted fan-structure just before the instability is shown above the graph. The higher the distributed shear stress applied the shorter the uncompleted fan-structure at the moment of instability start and the greater the rupture speed and rupture violence.

FEATURES OF THE FAN-MECHANISM ACTIVATION IN LABORATORY SPECIMENS AND IN NATURAL ROCK MASS

It should be noted that loading conditions causing the fan-mechanism generation and propagation in rock specimens in laboratory are quite specific. In the physical model the fan-head was generated by a locally applied high stress while the distributed shear stress along the future fault was low. In rock specimens tested at highly confined compression such situation is not achievable due to very small specimen sizes. In order to generate the fan-structure in a rock specimen the whole specimen has to be loaded axially up to high stresses that correspond to the material strength τ_u (point P on a stress-displacement curve in Fig. 5b). Acoustic emission studies (e.g. Lei at al., 2000) show that in hard rocks under highly confined compression the localized shear fracture development starts close to the peak strength (point S on the curve). The pre-peak stage between points S and P is associated with development of the first half of the fan-structure.
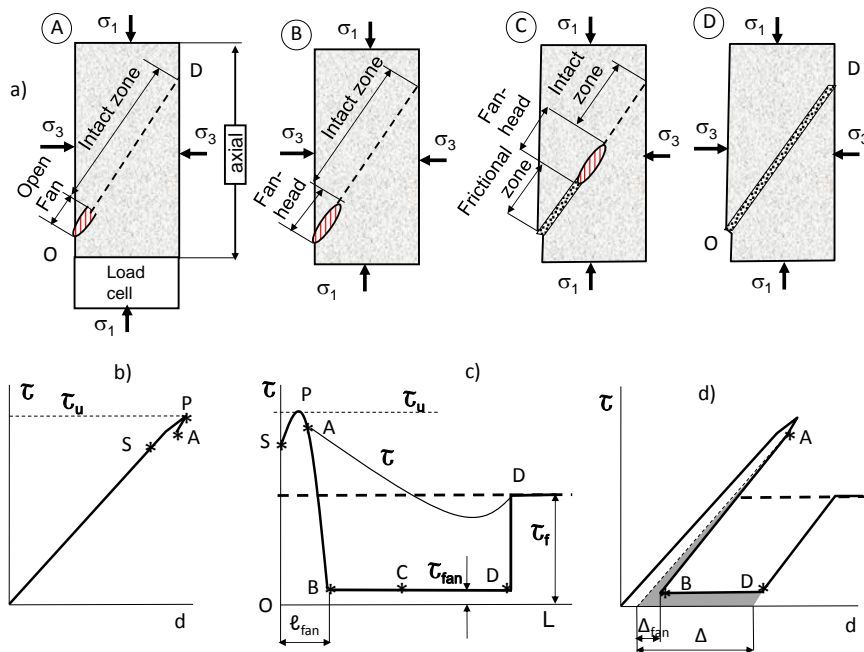

Figure 5. Features of the fan-mechanism activation in laboratory specimens at highly confined compression

At point P, when the first half of the fan has completed, the distributed shear stress in the specimen along the future shear rupture, shown by dotted line in Fig. 5a-A, is equal to τ_u. It means that point P represents the point of instability for the developing fan-structure. This is true, however, for the idealized fan-structure. In real materials different imperfections (e.g. friction in joints of rotating domino-blocks, partial collapse of domino-blocks at rotation) make it possible to provide controllable

failure at the beginning post-peak stage until point A on the curve in Fig. 5b. It should be noted again that the controllable post-peak part (PA) becomes shorter with rising confining pressure (see Fig. 2a). It happens because the imperfection of domino-structure decreases with rising σ_3. The question will be discussed further.

During spontaneous failure after point A shear resistance and displacement along the developing fault OD in Fig. 5a is very irregular. Three specific zones can be distinguished: 1) the fan-head zone where the failure process and domino-block rotation is in progress; 2) the frictional zone located behind the fan-head where the blocks have completed their rotation and the full friction is mobilised; and 3) the intact zone in front of the fan-head. A load cell and an axial gauge in Fig. 5a mounted on the specimen as is commonly used in experiments can only measure the average load-bearing capacity and displacement of the specimen during the failure process. Results obtained on the basis of these gouges do not allow estimating real material strength and energy balance of the failure process. However, the new knowledge about the fan-mechanism gives us a chance to derive this inaccessible information.

Fig. 5c shows the situation along the developing fault OD in the specimen. The curve SPBD reflects shear resistance of the fan-structure. The dotted horizontal line corresponds to the frictional strength τ_f. The curve AD shows variation in the average shear resistance of the specimen during the failure process measured by the load cell. Despite the fact that the average shear resistance of the specimen is quite high the actual material strength during the failure process is determined by the shear resistance of the fan-structure. Between points A and B the fan-structure formation occurs in dynamic regime. Between points B and D the completed fan-head with shear resistance of τ_{fan} crosses the specimen. At this stage of the failure process the actual material strength has the minimum value corresponding to τ_{fan}. After completion of the failure process strength of the material (specimen) is determined by frictional strength τ_f of the created fault. The post-peak part of stress-displacement curve in Fig. 5d reflects the real variation of the material strength determined by the fan-mechanism during the spontaneous failure. The shaded area here corresponds to the real rupture energy.

It should be emphasized that during spontaneous failure after point A self-unbalancing conditions within the fan-head take place at any level of stresses above τ_{fan}. It means that stable and controllable failure beyond point A is principally impossible. This explains the absence of post-peak curves obtained at the controllable regime on hard rocks (UCS > 250 MPa) at highly confined compression.
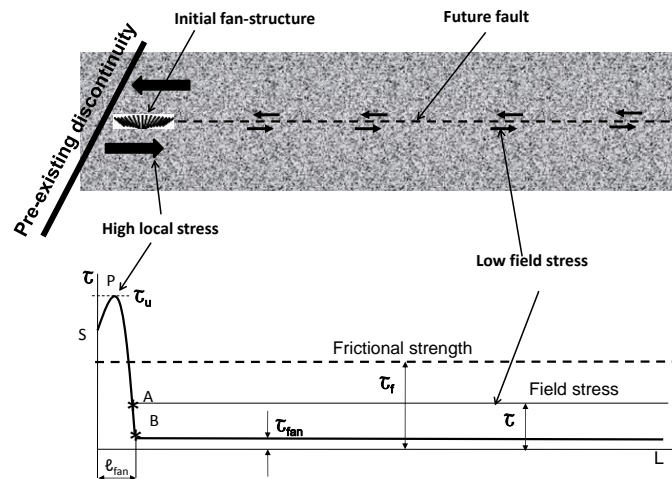

Figure 6. Features of the fan-mechanism activation in natural rock mass in the vicinity of pre-existing discontinuities

Fig. 6 illustrates features of the fan-mechanism activation in natural conditions. It is known that the field stress in the lithosphere cannot exceed the frictional strength. However, local stresses in intact rock mass in the vicinity of pre-existing discontinuities (e.g. boundaries between tectonic plates, faults, deep mines, etc.) can reach the fracture strength levels τ_u. According to the new approach, pre-existing discontinuities play the role of stress concentrators creating the starting conditions for the fan-

8

mechanism, but instability (e.g. earthquakes) occurs due to the development of new faults in the intact rock mass.

Fig. 6 illustrates this phenomenon. Fig. 6a shows a fragment of the rock mass with the local zone of high shear stress adjoining a pre-existing discontinuity where the fan-structure is generated and a large zone of lower stress where the fan-head can easily propagate. In Fig. 6b the horizontal dotted line shows the level of frictional strength τ_f along the future fault. The horizontal thin solid line corresponds to the field stress level τ. The thick solid graph illustrates shear resistance of the fan-head at two stages: nucleation (length of fan-head fracture ℓ_{fan}, strength τ_u) and propagation (length of created shear fracture $L \ggg \ell_{fan}$, strength τ_{fan}). The fan formation can be stable until point A if the local stress does not exceed the shear resistance of the developing fan-structure. However, after point A the fan-structure becomes in the self-unbalancing condition and the fan-head starts propagating spontaneously. The completed fan-head will propagate further dynamically through the intact rock mass extending the new fault and causing earthquake.

Paradoxically low strength of intact rock provided by the fan-mechanism favours the generation of new faults in an intact rock mass in preference to frictional stick-slip instability on pre-existing faults for which stresses above τ_f are required. This unique feature of the fan mechanism allows the supposition that the majority of dynamic events in the Earth's crust result from the generation of new faults. By creating new faults the fan-mechanism increases the intensity of rock fracturing in earthquake active zones, making these zones finally riddled with faults. The new approach explains the spatial distribution of earthquakes: new faults are generated in intact rock at new locations. However, the proximity of the pre-existing discontinuities to the area of instability caused by the fan-mechanism creates the illusion of stick-slip instability on the pre-existing faults, thus concealing the real situation.

The fan-mechanism can be responsible for some types of man-made earthquakes. Special studies conducted in South African mines (Gay and Ortlepp, 1979; McGarr et al., 1979) show that shear rupture rockbursts, which are seismically indistinguishable from natural earthquakes, are generated in intact hard rock (dry quartzite) in zones of highly confined compression. It was shown that these mine tremors and earthquakes share the apparent paradox of failure at low shear stresses, while laboratory measurements indicate high material strengths.

VARIABLE EFFICIENCY OF THE FAN-MECHANISM

Eq. (1) shows that increasing the ratio r/w decreases the effect of friction in joints on the fan shear resistance: the higher the r/w the greater efficiency of the fan-mechanism. As was discussed previously, the length of the domino-blocks is a function of confining pressure σ_3 (dotted line ℓ *versus* σ_3 in Fig. 2c). By analogy, the dotted line in Fig. 7a shows symbolically the variation of the ratio r/w *versus* σ_3 within the pressure range between $\sigma_{3min(shear)}$ and $\sigma_{3max(hinge)}$. This line indicates the variation in hinge efficiency with confining pressure if the domino-blocks do not collapse at rotation. In natural conditions, however, blocks can collapse.
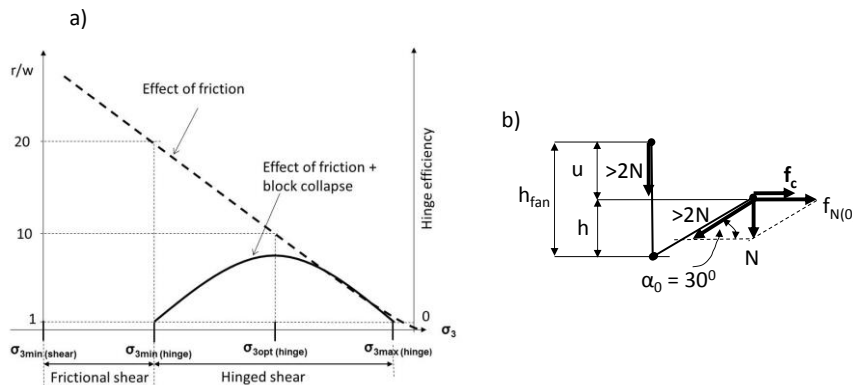

Figure 7. Variation of the fan-mechanism efficiency versus confining pressure caused by domino-blocks collapse at rotation

Each block in the fan works similar to a beam with rotation-free end conditions loaded along the beam axis. Fig. 7b illustrates features of the axial loading of a block at the initial ($\alpha_0 = 30^0$) and vertical positions. It shows that the value of axial force applied to the front domino-block is more than twice the elementary force N (associated with the evenly distributed normal stress σ_n). This means that any block at the front position is in the most stressed conditions. If the block does not collapse at the start of rotation it will be capable of bearing identical stresses at any stage of its rotation, including the vertical position, when it deforms the rupture faces by the value u. All blocks of the fan in combination create additional normal stresses moving apart the fault faces (wedge effect). We can suppose that during rotation from the initial to the final position, each domino-block of the completed fan-structure is under approximately the same axial stresses.

In rocks under confined compression, domino-blocks are subjected to high loads which can lead to buckle and collapse of the blocks. On the basis of information presented in (Megahid et al., 1993) we assume that domino-blocks with slenderness ratio r/w $\leq$ 10 are stable at axial loading. Domino-blocks with slenderness ratio r/w > 10 will be subjected to destruction to different degrees, depending on the ratio r/w. The solid curve in Fig. 5a illustrates a possible variation of the fan-mechanism efficiency versus confining pressure σ_3, taking into account the block destruction. At values r/w < 10 the efficiency varies in accordance with Eq. (1). Within the range 10 < r/w < 20, owing to different degrees of destruction (depending on r/w), only a part of each block can maintain stability operating as a hinge. Very long blocks with slenderness ratio r/w > 20 completely collapse on rotation, resulting in gouge and common friction between the interfaces. This is a preliminary explanation for the variable fan-mechanism efficiency. Further experimental and theoretical studies will allow better understanding of the features of this phenomenon.

The important point is that the fan-mechanism is active only within the range of confining pressure between $\sigma_{3min(hinge)}$ and $\sigma_{3max(hinge)}$, with optimal efficiency at $\sigma_{3opt(hinge)}$. The variable efficiency of the fan-mechanism with confining pressure (or depth) causes corresponding (unconventional) variation in rock brittleness (see Fig. 1c) and similar variation in rock strength. In accordance with Eq. (1) shear resistance (strength) of the fan-head for domino-blocks characterised by the ratio w/r = 0.1 is one-tenth the frictional strength: $\tau_{fan} \approx 0.1\tau_f$. This means that at this ratio rocks exhibit the minimum strength provided by the fan-mechanism operating with optimal efficiency. It was shown in Tarasov (2010), Tarasov and Randolph (2011) that the optimal efficiency of the fan-mechanism for very hard rocks can be reached at confining pressures above 300 MPa which corresponds to depths of maximum earthquake activity.

DEPTH DISTRIBUTION OF THE LITHOSPHERIC STRENGTH AND EARTHQUAKE ACTIVITY CAUSED BY THE FAN-MECHANISM

The domino structure and the fan-shaped rupture head can be formed in small primary ruptures and in large segmented faults. Features of the fan-structure formation in large segmented faults was discussed in Tarasov (2014). The fan-structure generated in any type of faults has the same extraordinary features introduced above. It was shown that the fan-mechanism efficiency is variable with confining pressure and consequently with depth. The discussed unique features of the fan-mechanism allow proposing a new understanding of the lithospheric strength and earthquake activity in the vicinity of pre-existing faults.

Fig. 8 illustrates the general idea about the role of the fan-mechanism in determination of the lithospheric strength and earthquake activity. It shows relative depth distributions between the following parameters: a) fan-mechanism activity, b) lithospheric strength, c) post-peak rock brittleness, and d) earthquake frequency (number of earthquakes). The schema of lithospheric strength in Fig. 8b incorporates curves of different types of strength: frictional, creep, fracture and fan strength. The curve of frictional strength corresponds to the lithospheric strength in accordance with the Byerlee's law (Byerlee, 1978). The fracture strength curve represents strength of intact rock. The fan-strength curve reflects the material strength determined by the fan-mechanism of variable efficiency (Tarasov, 2013). The maximum efficiency of the fan-mechanism defines the depth-position of the minimum fan-strength and the maximum of rock brittleness and earthquake frequency.
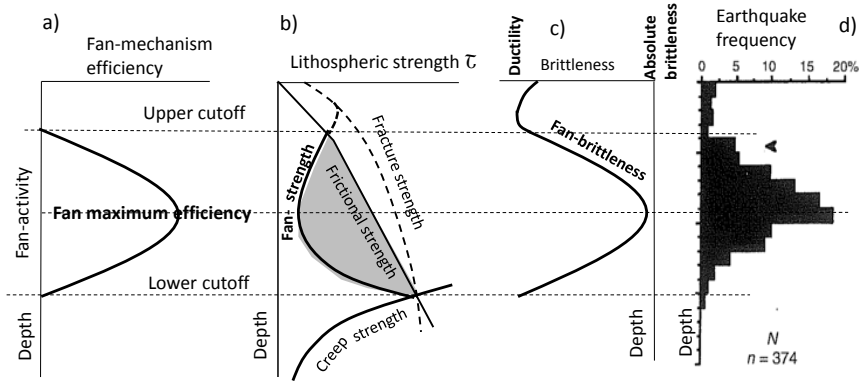
Figure 8. Relative depth distribution of: a) fan-mechanism activity; b) lithospheric strength; c) post-peak rock brittleness; and d) earthquake frequency (the histogram from Scholz (2002))

Fig. 8b shows that at shallow depths frictional strength along pre-existing faults represents the lower limit of rock strength and determines the lithospheric strength. Within the depth region where fan-strength is less than frictional strength the situation is very specific. The fan-strength curve indicates potential lithospheric strength corresponding to shear resistance of the fan-mechanism. Before activation of the fan-mechanism the lithospheric strength is determined by the frictional strength. However, after generation of the fan-head by high local stress the dynamic development of a new fault can occur at any level of the field stress within the gray area located between the frictional and fan-strength curves. The closer the level of field stress to the frictional strength the more violent the failure process is. Earthquakes associated with stick-slip instability along pre-existing faults can occur if the field stress exceeds the frictional strength.

The new concept comprising two forms of instability caused by the fan-mechanism and by the conventional stick-slip mechanism provides more comprehensive understanding of lithosphere strength and earthquake instability and can explain a number of earthquake features which previously had not been fully resolved.

CONCLUSIONS

The paper introduces the recently identified fan-structure dynamic shear rupture mechanism generated in intact hard rocks at highly confined compression, the most important features of which are:
- In the fan-mechanism, the rock failure associated with consecutive creation of small slabs (domino-blocks) from the intact rock in the rupture tip is driven by the self-unbalancing fan-shaped domino structure representing the rupture head.
- The mechanism can develop new dynamic faults in intact rock mass at shear stress levels significantly less than frictional strength;
- For the initial formation of the fan-head high local stresses are required.
 On the basis of these unique features of the fan-mechanism a new approach in understanding of the lithospheric strength and earthquake activity is proposed. Accoring to the new approach pre-existing discontinuities in the Earth's crust play the role of local stress concentrators providing the initial formation of the fan-head in the adjoining intact rock mass. Further dynamic creation of a large new fault (earthquake) can occure at low shear stresses even below the frictional stregnth. Paradoxically low strength of intact rock provided by the fan-mechanism favours the generation of new faults in the intact rock mass adjoining the pre-existing fault in preference to frictional stick-slip instability along the pre-existing fault. The varying efficiency of the fan-mechanism with depth provides a specific depth distribution of lithospheric strength and earthquake activity.

REFERENCES

Brace WF and Kohlstedt D (1980) "Limits on lithospheric stress imposed by laboratory experiments", *Journal of Geophysical Research*, 85, 6248-6252.

Byerlee JD (1978) "Friction of rocks", *Pure Appl. Geophys*, 116:615-626.

Gay N C, Ortlepp W D (1979) "Anatomy of a mining-induced fault zone", *Geol. Soc. Am. Bull*., 90, 47-58.

Heaton TH (1990) "Evidence for and implications of self-healing pulses of slip in earthquake rupture" *Physics of Earth Planet International* 64(1), 1-20.

Horii H and Nemat-Nasser S (1985) "Compression-induced microcrack growth in brittle solids: Axial splitting and shear failure", *J Geophys Res*, 90: 3105-25.

King GCP, Sammis CG (1992) "The mechanisms of finite brittle strain" *PAGEOPH*, 138, 4, 611-640.

Lei X, Kusunose K, Rao MVMS, Nishizawa O, Satoh T (2000) "Quasi-static fault growth and cracking in homogeneous brittle rock under triaxial compression using acoustic emission monitoring", *J Geophys Res*, Vol. 105. No. B3: 6127-6139.

Lykotrafitis G, Rosakis AJ, Ravichandran G (2006) "Self-healing pulse-like shear ruptures in the laboratory" *Science* 313, 1765-1768.

McGarr A, Spottiswoode SM, Gay NC, Ortlepp WD (1979) "Observations relevant to seismic driving stress, stress drop, and efficiency", *J. Geophys. Res*. 84, 2251-2261.

Megahid AR, Soghair H, Hageed MAA, Hafer AMAA (1993) "Strength and deformation capacity of slender RC beams" *In Proceedings Fracture and Damage of Concrete and Rock – FDCR-2.*

Ohnaka M, Kuwahare Y, Yamamoto K, Hirasawa T (1986) "Dynamic breakdown processes and the generating mechanism for hi-frequency elastic radiation during stick-slip instabilities" *Earthquake Source Mechanics, Geophys. Monogr. Ser.,* vol. 37, edited by S.Das, J. Boatwright, and CH Scholz, pp. 13-24, AGU, Washington, D.C.

Peng S, Johnson AM (1972) "Crack growth and faulting in cylindrical specimens of Chelmsford granite", *International Journal of Rock Mechanics and Mining Science* 9, 37-86.

Reches Z, Lockner DA (1994) "Nucleation and growth of faults in brittle rocks" *Journal of Geophysical Researcn* 99, No. B9, 18159-18173.

Scholz CH (2002) <u>The mechanics of earthquakes and faulting</u>, Cambridge: Cambridge University Press.

Stavrogin AN, Tarasov BG (2001) <u>Experimental physics and mechanics of rock</u>, Balkema, Amsterdam.

Tarasov BG (2010) "Superbrittleness of rocks at high confining pressure", *Fifth International Seminar on Deep and High Stress Mining,* Santiago, Chile, 119-133.

Tarasov BG, Randolph MF (2011) "Superbrittleness of rocks and earthquake activity", *International Journal of Rock Mechanics and Mining Science* 48: 888-898.

Tarasov BG (2013) (Depth distribution of lithospheric strength determined by the self-unbalancing shear rupture mechanism", *Eurock 2013, Rock Mechanics for Resources, Energy and Environment* ed. Marek Kwasniewski and Dariusz Lydzba. 165-170.

Tarasov BG, Potvin Y (2013) "Universal criteria for rock brittleness estimation under triaxial compression" *International Journal of Rock Mechanics and Mining Science* 59: 57-69.

Tarasov BG, Guzev MA (2013) "New insight into the nature of size dependence and the lower limit of rock strength", *8th International Symposium on Rockbursts and Seismisity in Mines*, Saint-Petersburg, 31-40.

Tarasov BG (2014) "Hitherto unknown shear rupture mechanism as a source of instability in intact hard rocks at highly confined compression", Tectonophysics, 621; 69-84.

Wawersik WR, Fairhurst C (1970) "A study of brittle rock fracture in laboratory compression experiments" *Int J Rock Mech Min Sc,* 7: 561-75.